Materials Research Bulletin 78 (2016) 148–157

Contents lists available at ScienceDirect

Materials Research Bulletin

journal homepage: www.elsevier.com/locate/matresbu

Impedance spectroscopy and conduction mechanism of $LiAlP_2O_7$ material

Y.Ben Taher[a,*], A. Oueslati[a], K. Khirouni[b], M. Gargouri[a]

[a] Condensed Matter Laboratory, University of Sfax, Faculty of Sciences, B.P. 1171, 3000 Sfax, Tunisia
[b] Laboratoire de Physique des Matériaux et des Nanomatériaux Appliquée à l'Environnement, Faculté des Sciences de Gabès, Tunisia

ARTICLE INFO

Article history:
Received 11 January 2016
Received in revised form 19 February 2016
Accepted 22 February 2016
Available online 24 February 2016

Keywords:
A. Ceramics
C. Impedance spectroscopy
C. Raman spectroscopy
C. X-ray diffraction
D. Electrical properties
D. Dielectric properties

ABSTRACT

$LiAlP_2O_7$ compound has been obtained by standard solid-state reaction technique and found to crystallize in the monoclinic system with $P2_{1/a}$ space group. The impedance plots are well fitted to two equivalent circuit models. The dc conductivity follows Arrhenius behavior with two different activation energies Ea (I) = 0.84 eV for $T < 610$ K and Ea(II) = 0.93 eV for $T > 610$ K. Actually, the values of activation energies obtained from the dc conductivity and the relaxation frequency are similar, and hence the transport in the titled compound can be described through a hopping mechanism, dominated by the motion of Li^+ ions. Besides, the frequency dependence of the conductivity is interpreted in terms of Jonscher's law. The NSPT model and the CBH model is the most applicable conduction mechanism in region (I) and (II), respectively. The ion transport is due to the hopping of Li^+ ions along [100] tunnels direction. The conduction mechanism is studied with the help of Elliot's theory, and the Elliot's parameters are determined.

1. Introduction

Various research areas are more and more interested in using the Phosphate-based materials. As a result, these materials have been the subject of several previous studies owing greatly to their interesting physical properties like piezoelectric, luminescence, catalysis, absorption, ionic conductors ferroelectric, fluorescent properties [1–6].

Extensive works have been carried out for the search of superior fast lithium-ion conductors as membrane in advanced batteries has been carried out [7–11]. It has been shown by Goodenough et al. that frameworks built up from PO_4 or from P_2O_7 polyedra are good candidates for the use of solid electrolytes [12] and electrode materials [13] in rechargeable lithium cells.

Among a wide variety of such materials researchers are more interested in lithium diphosphates ceramics $LiMP_2O_7$ (M: transition metal), which have attracted researchers' interests thanks to its original physical properties. Among these properties, we can mention the high mobility of lithium ions which promotes the insertion/extraction reactions.

In this aim, we are interested, in our laboratory, to investigate the physical properties of diphosphate materials with the general formula $LiM^{III}P_2O_7$. These material attracted researchers' interests thanks to its original physical properties. Among these properties, we can mention the high mobility of lithium ions which promotes the insertion/extraction reactions. In the last years, the AC conductivity and dielectric properties of $LiFeP_2O_7$ and $LiCrP_2O_7$ compounds have been reported [14,15].

For instance, the present research work selected a new category of lithium intercalating cathode candidates, since no reports are available in literature that studied the electrical properties. $LiAlP_2O_7$ is isotypic with $LiFeP_2O_7$ [16], and it is one of the monoclinic systems with the space group P21/a.

Hence, the purpose of the present work is to determine the equivalent electrical circuit which can model the experimental data and characterize the electrical microstructure via impedance spectroscopy in a wide range of frequencies and temperatures. The measurements of AC conductivity have been widely used to understand the conduction process in materials.

2. Experimental part

Synthesis of powder of $LiAlP_2O_7$ diphosphate was carried out by the standard solid-state reaction techniques. Stoichiometric quantities of Li_2CO_3, Al_2O_3 and $NH_4H_2PO_4$ were ground, mixed and progressively heated first to 573 K and then to 1073 K. X-ray powder diffraction pattern was recorded using a Philips PW 1710 diffractometer operating with copper radiation $K\alpha = 1.5418$ Å.

---

[*] Corresponding author.
E-mail address: youssef.btaher@yahoo.fr (Y.B. Taher).

http://dx.doi.org/10.1016/j.materresbull.2016.02.033

Unit cells parameters of the synthesis compound have been refined by the least square method from the powder data. Raman scattering investigation was performed on powder, using a spectrometer type Horiba Jobin–Yvon T64000.

The impedence spectroscopy measurements were performed on pellet discs of about 8 mm in diameter and about 1.2 mm in thickness. Electrical impedence was measured in the frequency range from 200 to 10 MHz.

3. Results and discussion

3.1. Crystalline parameters

The room temperature XRD pattern of the $LiAlP_2O_7$ compound is shown in Fig. 1. In fact, all the X-ray peaks were indexed in the monoclinic system with P21/c space group. The refined unit cell parameters are a = 4.81 (3) Å, b = 8.09 (2) Å, c = 6.96 (2)Å, $\alpha = 90°$, $\beta = 109.22°(3)$.

The $LiAlP_2O_7$ structure is characterized by straight wide tunnels along the a-axis in the network built of the AlO_6 octahedra and the PO_4 tetrahedra sharing corners (Fig. 2). The tunnels along the a-axis are edged by four tetrahedra and three octahedra. Li+ ions are located in the voids of the tunnels. The PO_4 tetrahedra are paired by one corner forming the diphosphate anion $[P_2O_7]^{4-}$. The projection along b axis is show in Fig. 3. The structure can be describe by an alternation of two types of layers stacked along [100] direction. The first layer formed by PO_4 tetrahedra and the second layers formed by AlO_6 octahedra.

3.2. Raman spectroscopy

The Raman spectrum of the $LiAlP_2O_7$ compound at room temperature is shown in Fig. 4. It reveals different peaks which can be attributed according to published results [17–19] in similar compound. The following sequence of diphosphate vibrations in decreasing frequency order:

$\upsilon_{as}(PO_3) > \upsilon_s\ (PO_3) > \upsilon_{as}\ (POP) > \upsilon_s\ (POP) > \delta_{as}(PO_3) > \delta_s(PO_3) > \delta_s(POP)$

υ_{as} and υ_s refer to the asymmetric and symmetric stretching vibrations, while δ refers to the binding vibrations.

In fact the bands observed in the 580–969 cm^{-1} region are attributed to the asymmetric and symmetric P–O–P stretching modes. Indeed the bands due to the symmetric and asymmetric binding vibrations of PO_3 are generally observed in the regions 200–575 cm^{-1}. Frequencies and assignments of Raman bands are given in Table 1.

3.3. Modulus study

Modulus formalism is generally used to analyze dielectric relaxation. The advantage of this representation is that the electrode polarization effects are minimized in this formalism. We can represent real dielectric relaxation process admitted as [20]

$$M = M' + jM'' = j\omega C_o Z \quad (1)$$

where M′ and M″ are the real and imaginary parts of complex modulus, C_0 is the vacuum capacitance of the cell, ω is the angular frequency, and Z is the complex impedance.

Fig. 5 shows the variation of the real part of the electric modulus M′ as a function of angular frequency at different temperatures. In the low frequency region M′ approaching to zero show that the electrode effect can be neglected in the modulus representation [21]. Moreover, the increase in the value of M′ with the frequency approaching eventually to $M_\infty = (1/\varepsilon_\infty)$, may be attributed to the conduction phenomena due to short-range mobility of charge carriers.

The variation of the experimental and simulated data of the imaginary part M″ of the modulus as a function of frequency at several temperatures is shown in Fig. 6. M″ increases with the frequency and reaches a maximum value which is linked to the bulk relaxation frequency (ω_p) and then decreases along with the temperature. On the other hand, the position of this peak shifts toward higher frequencies with the increase in temperature suggesting an ionic conductor character of the sample [21]. The general method to check the nature of the relaxation in the solid is to fit the measured data by Kohlrausch Williams Watts (KWW) et al. They have been recently proposed by Bergman [22].

$$M' = \frac{M'_{max}}{\left[(1-\beta) + \left(\frac{\beta}{1+\beta}\right)\left(\beta\left(\frac{\omega_{max}}{\omega}\right) + \left(\frac{\omega}{\omega_{max}}\right)^{\beta}\right)\right]} \quad (2)$$

where M''_{max} is the peak maximum and ω_{max} is the peak frequency of the imaginary part of the modulus and β is exponent.

On the other hand, the variation of the relaxation frequency ω_p with temperature, in inset Fig. 6, follows the Arrhenius relation. This plot reveals the existence of two activated relaxation processes in the temperature ranges of T < 610 K (phase I) and T > 610 K (phase II). The obtained activation energies are equal to 0.82 eV below 550 K and 0.94 eV above this temperature.

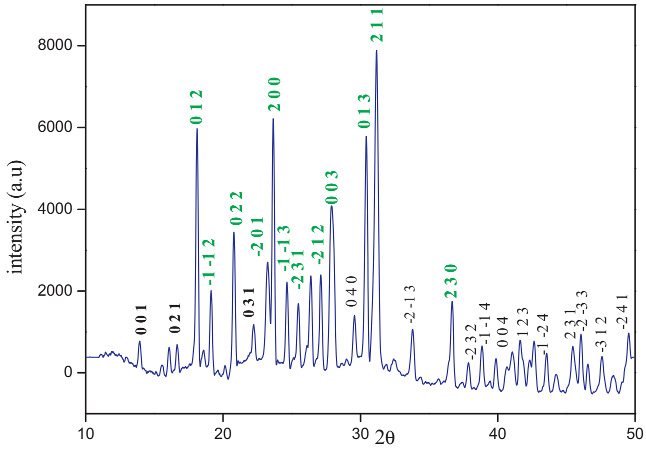

Fig. 1. X-ray powder diffraction pattern for $LiAlP_2O_7$.